Acta Cryst. (1992). B48, 747–752

From Crystal Structure Data Towards Reaction Paths in the Solid State?

BY A. VEGAS AND M. MARTÍNEZ-RIPOLL

UEI de Cristalografía, Instituto Rocasolano, CSIC, Serrano 119, *E*-28006 *Madrid, Spain*

(*Received* 17 *January* 1992; *accepted* 15 *April* 1992)

Abstract

The structures of FeB, GdSi, Re_3B, Ni_2In and δ-Ni_2Si are analyzed on the basis of their parent metal structures which become modified during compound formation. The observed metallic fragments maintain the original topology and distances, and the small distortions observed in them do not occur randomly, but are correlated as in molecular compounds. This analysis is not only used to describe the structures in a simpler way, but also to infer plausible reaction mechanisms in the solid state.

Introduction

Metal clusters have been widely studied and much of the work, aimed at correlating physical properties with structural and bonding aspects, has been collected in reviews (Franzen, 1978; Jansen, 1987; Simon, 1981, 1988; Hughbanks, 1989).

Until recently, the existence of metal clusters was seen as a logical feature in interstitial compounds, which were considered as bulky metals, slightly distorted by the inclusion of small amounts of other atoms (see Wells, 1975). This was also true of the so-called metal-rich compounds, in which the unsaturated valences of the metal atoms are used to form metal–metal bonds. As examples of the latter we may mention Fe_3C (Lipson & Petch, 1940) and $Cs_{11}O_3$ (Simon, 1988), both clearly related to Fe and Cs metals, respectively.

These bonding aspects led Franzen (1978) to consider the metal-rich compounds as modified metals in which the metallic interactions are partially modified as the result of metal–nonmetal bonding. Other examples of relating the metal substructure to the parent metal can be found in the articles of Simon (1981, 1988), dealing with structure and bonding in clusters of metal-rich compounds and clusters of valence-electron-poor metals. More explicit references to such a relationship can be found in the articles dealing with d^{10} metal aggregates (see Jansen, 1987) and in an article devoted to the bonding in clusters and condensed clusters of early transition and rare-earth metals (Hughbanks, 1989).

However, in an independent way, and looking for an alternative to the model of O'Keeffe & Hyde (1981, 1985) for describing crystal structures, we have shown that the relationship between the structure of the parent metal and the metal substructure in a given compound is not restricted to compounds with unsaturated bonding. It also appears in compounds with saturated valences [apatite: $Ca_5(PO_4)_3(OH,F)$, olivine: Mg_2SiO_4, *etc*], even in compounds traditionally considered as ionic ($KClO_3$) or those such as TiO_2, which is far from being considered a metal-rich compound (Vegas, Romero & Martínez-Ripoll, 1990, 1991). For some of the structures discussed there, a possible reaction mechanism was advanced in the sense that metallic fragments observed in many structures could be seen to be the result of a process of either dynamic deformation or breaking up, initiated in the parent metal.

In the present work we apply this model to simple binary compounds such as FeB, GdSi, Re_3B, Ni_2In and δ-Ni_2Si in order to deduce a plausible reaction path from the examination of the metallic fragments appearing in them.

Discussion

The FeB *structure and elemental* Fe

Iron presents the phases collected in Table 1 (Landolt-Börnstein, 1971). The FeB structure (Hendricks & Kosting, 1930) is orthorhombic, *Pnma*, with $a = 5.495$, $b = 2.946$ and $c = 4.053$ Å, and is represented in Fig. 1(*a*). The classical description consists of columns of face-sharing Fe_6 trigonal prisms running parallel to the *b* axis. The columns are linked by additional edge-sharing. The B atoms are off-center of these trigonal prisms. Parthé (1981) has described the structure as a twinned h.c.p. arrangement of Fe atoms with boron in the trigonal prisms generated at the twin plane. O'Keeffe & Hyde (1985) have related this structure to the cation arrays of many sulfates, selenates, chromates, *etc*.

Our alternative description is based on the space between trigonal prisms (shaded in Fig. 1*a*). These apparently empty holes are really fragments of a body centered cubic net, the Fe—Fe distances being within a few percent of those of the high-temperature b.c.c. phase of metallic iron. The fragments are easily

0108-7681/92/060747-06$06.00

Table 1. *The known phases of iron*

Phase	Lattice	Cell dimensions (Å)	Shortest Fe—Fe distances (Å)
α	b.c.c.	$a = 2.866$	2.48
δ	b.c.c.	$a = 2.932$	2.54
λ	f.c.c.	$a = 3.647$	2.58
ε	h.c.p.	$a = 2.465$, $c = 4.050$	2.465

recognizable if we look at Fig. 1(*b*) which represents a b.c.c. net, projected onto (001), divided into such fragments. One of them is also shaded as in Fig. 1(*a*) for comparison.

The conversion of the δ-Fe net into the FeB structure can be accomplished by a cooperative rotation of these fragments around the [001] axis, where only two of the eight Fe—Fe bonds are broken or lengthened whereas the other six remain almost equal to those of elemental Fe. This mechanism is illustrated in Figs. 1(*c*) and 1(*d*) which represent two intermediate steps. In the first one, the fragments of Fig. 1(*b*) move parallel to [100] to give the pattern represented in Fig. 1(*c*). As a consequence, two Fe—Fe bonds are broken and trigonal prisms (dotted lines in Fig. 1*c*) are formed. In a second step, the relative displacements of the two-dimensional blocks (marked with arrows in Fig. 1*c*), give rise to the pattern of Fig. 1(*d*), which is comparable to the Fe substructure of FeB (Fig. 1*a*). A final comment should be made about the metal–metal distances in both FeB and Fe. In the former, the iron blocks are defined by the distances *d*, *e*, *f* and the *b* axis of the unit cell (see Fig. 1*d*). Their values are $b = 2.947$, $d = 2.927$, $e = 2.620$ and $f = 2.667$ Å. The two *b* and two *d* distances define a square which would correspond to the $(100)_{b.c.c.}$ faces and compare well with the unit-cell parameters of the α- and δ-phases of iron ($a = 2.866$ and 2.932 Å, respectively). On the other hand, the four distances $2e$ and $2f$ (2×2.62 and 2×2.667 Å respectively) are 7% longer than the expected value of 2.48 Å in α-Fe and 4% longer than the value of 2.54 Å in the δ-phase. However, the quoted distances are in better agreement with the shortest Fe—Fe distances in the f.c.c. γ-Fe. We can conclude that the iron array in FeB adopts an intermediate structure between the two iron phases, the b.c.c. and f.c.c. (really, the body-centered tetragonal cell derived from it). To check this, we have applied the principle derived by Bürgi (1975) for isolated molecules or atomic groups, *i.e.* small distortions of tetrahedral MX_4 groups always occur under the condition that the sum of the four M—X distances remains approximately constant. In our case, the sum $\sum = 2d + 2b + 2e + 2f = 22.44$ Å is close to the corresponding values for α-, δ- and γ-Fe (21.38, 21.89 and 22.77 Å respectively). Moreover, it almost equals the mean value (22.33 Å) of δ- and γ-Fe (b.c.c. and f.c.c. respectively), a very nice coincidence which seems to indicate that distortions are also correlated in metallic groups.

In the same way, the isostructural GdSi (Nagaki & Simon, 1990) can be thought of as being derived from the b.c.c. Gd net ($a = 4.05$ Å and Gd—Gd distances of 3.52 Å). In this case, the $(100)_{b.c.c.}$ contacts suffer a rectangular distortion (3.858 Å ×

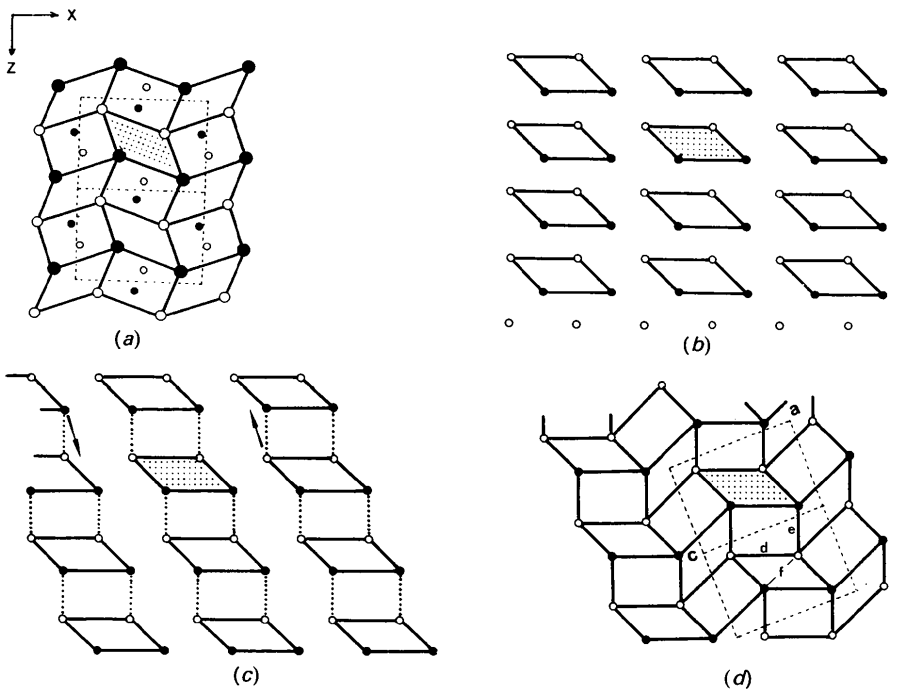

Fig. 1. Derivation of the FeB structure from the b.c.c. δ-Fe net. (*a*) The real structure of FeB projected onto the *ac* plane. The shaded area corresponds to a fragment of a b.c.c. net. Small and large circles represent B and Fe atoms, respectively. Open and full circles are shifted by *b*/2 with respect to each other. (*b*) A b.c.c. net, viewed along [100], divided into fragments such as those appearing in (*a*). (*c*) Pattern obtained from (*b*) by relative displacement of rows of blocks, parallel to [100]. Arrows indicate the further shifts which are needed in order to obtain the next drawing. (*d*) The idealized Fe substructure, to be compared with that of FeB. References to the distances *d*, *e* and *f* are given in the text.

4.281 Å) but the mean value (4.07 Å) almost equals the a value in the pure metal. The other four distances (2×3.643 Å and 2×3.689 Å) are 4% longer than the expected value of 3.52 Å and are in better agreement with the value of 3.64 Å of h.c.p. Gd. However, the corresponding $\sum$ values, 33.40, 30.30 and 30.96 Å, for h.c.p. Gd, b.c.c. Gd and GdSi respectively, justify the choice of the cubic phase as reference.

Re_3B *and the structure of h.c.p.* Re

The only known phase for Re is h.c.p., with $a = 2.7609$ and $c = 4.4576$ Å (Landolt-Börnstein, 1971) and is shown projected onto (110) in Fig. 2(*a*). Re_3B is orthorhombic, *Cmcm*, $a = 2.890$, $b = 9.313$, $c = 7.258$ Å (Aronsson & Rundquist, 1962). The structure is shown in Fig. 2(*a*), projected onto the *bc* plane. It has been described in terms of isolated columns of base-sharing Re_6B trigonal prisms running parallel to the *a* axis, whose bases are isosceles triangles (2.72 and 2×3.04 Å), their height being 2.89 Å. The structure also presents short contact distances (ranging from 2.66 to 2.78 Å) between adjacent prisms. As with FeB, the structure has also been described by Parthé (1981) as a twinned h.c.p. array of Re atoms in which trigonal prisms are formed on the twin plane, following the concept of periodic unit-cell twinning of Andersson & Hyde (1974).

Our alternative point of view is that the Re array in Re_3B is a distorted h.c.p. array of rhenium, but in such a way that the observed twinning should be the result and not the origin of this structure type. The first observation is that the interprism Re—Re distances are shorter than two of the distances (2×3.04 Å) defining the prisms. Thus, it seems to us more realistic to define Re blocks showing a more homogeneous range of distances (from 2.72 to 2.89 Å), in better agreement with those of metallic rhenium (2.76 Å) and where the topology of the metal is maintained. Note also how the *c* axis of h.c.p. Re (4.46 Å) remains unaltered (4.41 Å) in the Re blocks. These are represented in Fig. 2(*a*), in contrast to the superimposed unit cell based on the trigonal prism description. The h.c.p. net of Fig. 2(*b*) has also been divided into such blocks, so that all Re atoms are involved in fragments of the same shape and size. From these drawings, it is easy to visualize how the h.c.p. net can be converted into the Re_3B structure by a cooperative rotation of the blocks, around the projection axis, to form trigonal prisms where the B atoms are located. This rotation should be equivalent to a two-step mechanism based on small displacements of the blocks as represented in Figs. 2(*b–d*). Displacement of rows of blocks, in the sense marked by arrows in Fig. 2(*b*), leads to the pattern in Fig. 2(*c*) and from this, by shearing in the sense of the arrows, one obtains the Re array of Re_3B (Fig. 2*d*). Compare this with the real structure of Fig. 2(*a*).

In order to achieve this, only two of the 12 Re—Re bonds per Re atom in the h.c.p. array would need to be broken or weakened to allow the displacive transition of a partially broken structure in which the defined fragments remain unaltered. So, considering only the Re atoms in Re_3B, the final coordination numbers are 10 + 1 and 10 + 2 for Re(1) and Re(2) respectively. The ten nearest are at distances ranging from 2.66 to 2.89 Å (mean 2.76 Å) for Re(1) and from 2.71 to 2.89 Å (mean 2.77 Å) for Re(2). Compare this with the value of 2.761 in metallic rhenium! The additional Re atoms, one and two respectively, are at 3.04 Å, which accounts for two of the distances forming the base of the trigonal prisms.

The Ni_2In *structure and h.c.p.* Ni

The known phases of Ni are: f.c.c. ($a = 3.524$ Å, Ni—Ni at 2.492 Å), b.c.c. ($a = 2.78$ Å, Ni—Ni at 2.41 Å) and h.c.p. ($a = 2.66$, $c = 4.32$ Å, Ni—Ni at 2.66, 2.65 Å). Ni_2In is hexagonal, $P6_3/mmc$, with $a = 4.185$, $c = 5.14$ Å (*Structure Reports*, 1942–1944, Vol. 9). The structure is represented in Fig. 3(*a*), projected onto (110). It has been described as columns of triangular base-sharing trigonal prisms, perpendicular to the projection plane, and further linked by edge-sharing into blocks parallel to the *c* axis. The aristotype, θ-Ni_2Si, has been described as a three-dimensional linkage of M_4X_6 clusters (see Simon, 1981). The metal atoms involved in these clusters correspond to those included in the shaded area of Fig. 3(*a*).

We view the Ni_2In structure as an h.c.p. Ni net, opened up by inclusion of the In atoms. The recognizable fragments are drawn in Fig. 3(*a*) and are also used to decompose the h.c.p. Ni net of Fig. 3(*b*). These fragments are larger than those defined by Simon (1981) for θ-Ni_2Si and, at the same time, are linked together to produce a three-dimensional array of Ni atoms, with Ni—Ni distances similar to those of hexagonal nickel. The h.c.p. Ni topology is maintained in each fragment but not in the whole array. Thus, it can be regarded as the result of an opening of the h.c.p. net where only some of the metal–metal bonds have been broken, the others remaining unaltered and serving as hinges (dotted lines in Fig. 3*b*) around which, the fragments rotate with respect to each other, in order to produce the pattern shown in Fig. 3(*c*). All Ni—Ni distances (see Fig. 3*c*) deviate from the ideal values of 2.65–2.66 Å. However, as in FeB, deviations from ideality are correlated in such a way that the sum of the eight

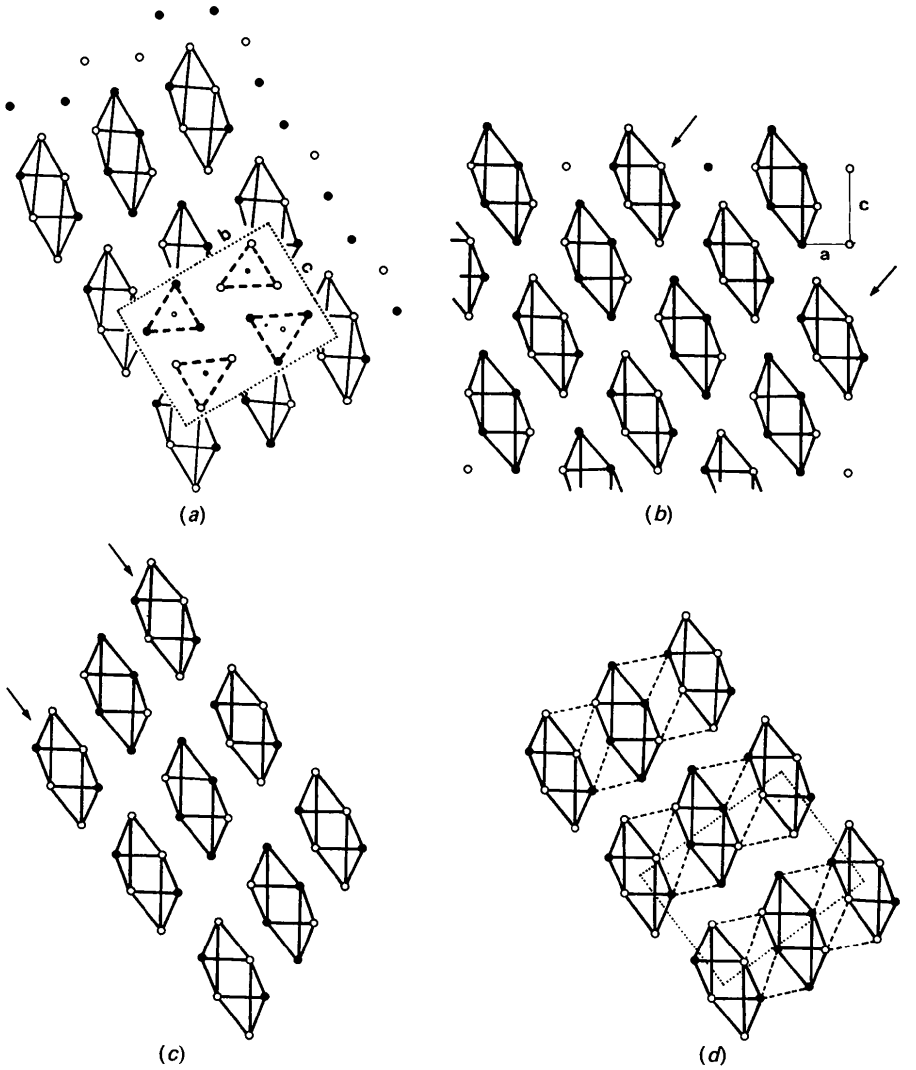

Fig. 2. Derivation of the Re_3B structure from h.c.p. Re. (*a*) The real structure of Re_3B, projected onto the *bc* plane, showing the columns of trigonal prisms. Large and small circles represent Re and B atoms respectively. Open and full circles are shifted *a*/2 with respect to each other. The unit cell is outlined over a set of h.c.p. Re fragments present in the structure. (*b*) The same fragments drawn on an h.c.p. Re net, projected onto (110). The *a* and *c* axes are marked. Arrows indicate the sense of displacement of these fragments in order to obtain the drawing (*c*). (*c*) Intermediate step with arrows indicating the relative shift of the blocks to arrive at the drawing (*d*). (*d*) Drawing of the idealized Re substructure to be compared with (*a*). The ideal unit cell is marked with dotted lines. Trigonal prisms are depicted with discontinuous lines.

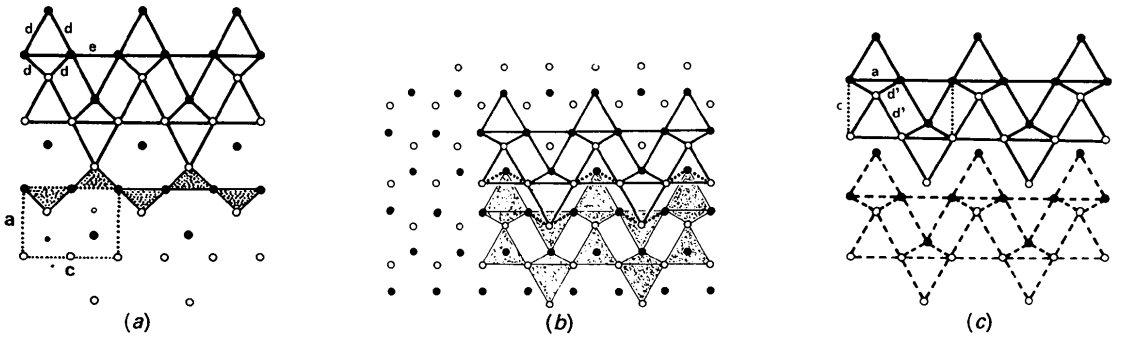

Fig. 3. The Ni_2In structure as derived from h.c.p. Ni. (*a*) The real structure of Ni_2In, projected onto (110), showing the chains of trigonal prisms. Open and full circles denote atoms shifted $\frac{1}{2}$ along the projection axis. Small and large circles are In and Ni atoms respectively. On the lower side, the unit cell is marked with dotted lines. Distances marked as *a*, *d* and *e* represent Ni—Ni bonds as referred to in the text. The upper side shows the largest metal fragment maintaining the topology of h.c.p. Ni. The shaded area shows the Ni clusters as defined by Simon (1981) in this structure type. (*b*) H.c.p. Ni divided into fragments similar to those described in (*a*). Dotted lines indicate the supposed hinges around which fragments would rotate to give the pattern shown in (*c*). (*c*) The idealized Ni substructure, to be compared with that of Ni_2In. The unit-cell borders are marked with dotted lines.

distances defining a $(100)_{h.c.p.}$ face and its capping atom, remains constant, within 1%. Thus, for Ni_2In, $\Sigma = 2e + 2a + 4d = 24.47$ Å (see Fig. 3*c*) and for h.c.p. Ni, $\Sigma = 2a + 2c + 4d' = 24.56$ Å. This is again a significant coincidence which indicates that distortions do not occur at random and that the choice of h.c.p. Ni as starting model is justified.

δ-Ni_2Si *and elemental* Ni

The structure of δ-Ni_2Si was reported by Toman (1952). It is orthorhombic, *Pbnm*, $a = 7.06$, $b = 4.99$, $c = 3.72$ Å, and is represented in Fig. 4(*a*), projected along [001]. It has been described in terms of columns of face-sharing Ni_6Si trigonal prisms, further connected by edge-sharing to form sheets parallel to (100). The sheets are shifted by $c/2$ with respect to each other. This structure type is adopted by other compounds, such as $PbCl_2$, Ca_2Si, *etc.*, and has been recognized in the cation array of many other oxygen-containing compounds such as β-Ca_2SiO_4, K_2SO_4, *etc.* (O'Keeffe & Hyde, 1985). As in the other examples discussed, the Ni—Ni distances, ranging from 2.54 to 2.72 Å, are similar to those in elemental nickel, without a clear difference between those involved in the trigonal prisms and those connecting them. The mean value $d = 2.62$ Å is longer than the expected value of 2.49 Å in f.c.c. Ni, and in the same way, the c axis is longer than the a axis of f.c.c. Ni. However, the ratio $d/c = 0.704 \simeq 2^{1/2}/2$ corresponds to an f.c.c. array. Thus, the Ni substructure can be regarded as interconnected fragments of a slightly expanded f.c.c. nickel as represented in Fig. 4(*b*). The same type of cluster has been used to describe Co_2P (Simon, 1981).

A closer inspection of the structure allows one to identify more extended f.c.c. Ni blocks, as represented in Fig. 4(*c*). These blocks are, in turn, interconnected by additional Ni—Ni bonds which are easily recognizable by comparing Figs. 4(*b*) and

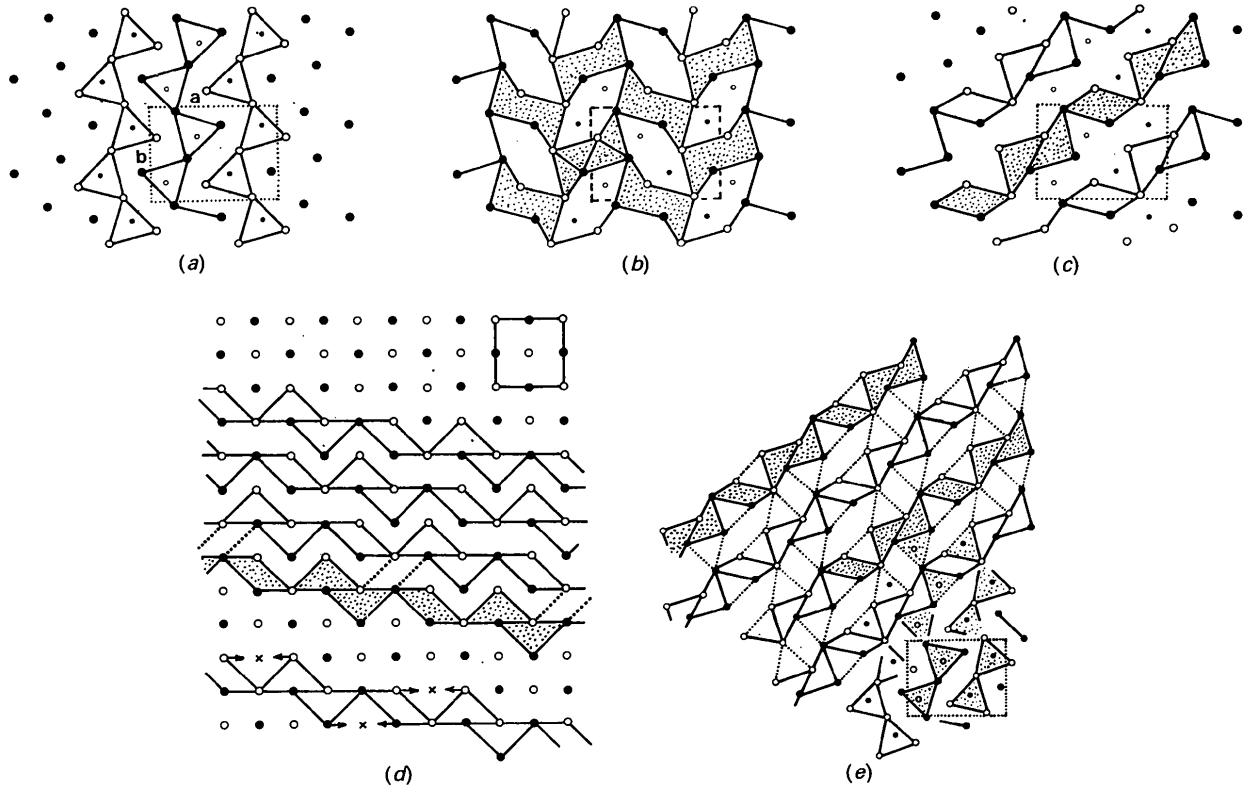

Fig. 4. The Ni substructure of δ-Ni_2Si derived from f.c.c. Ni. (*a*) The real structure of δ-Ni_2Si, described in terms of trigonal prisms. The unit cell is shown by dotted lines. Large and small circles represent Ni and Si atoms respectively. Open and full circles are shifted by $c/2$. (*b*) The same projection but described in terms of a linkage of Ni clusters, with f.c.c. topology, as defined by Simon (1981). (*c*) Alternative description in terms of infinite fragments (Ni sheets) running parallel to (110). (*d*) F.c.c. Ni viewed along [100] and divided into fragments similar to those defined in (*c*). One of them has been shaded for comparison. On the lower side, arrows indicate the direction of approach in order to give the real geometry appearing in (*c*). Crosses indicate the missing atoms. Dotted lines between sheets represent the unaltered bonds which would act as hinges. (*e*) Idealized reconstruction of δ-Ni_2Si from the sheets of (*d*) to be compared with (*a*). The ideal unit cell is marked with dotted lines on the lower side.

4(*c*). We believe that this alternative description allows a better representation of a possible reaction path which, starting from f.c.c. Ni, leads to the structure under discussion by a cooperative displacement of the blocks. Fig. 4(*d*) is an f.c.c. lattice divided into these blocks, in such a way that every atom of the net belongs to identical fragments. In the lower part of Fig 4(*d*) one of these fragments is drawn with arrows indicating the atomic displacement needed to form the real fragments appearing in δ-Ni_2Si (Fig. 4*c*). In other words, if the Ni structure is broken up into such fragments, the atoms marked with arrows would approach each other at a distance similar to that formed with the 'missing' atom, forming the trigonal prisms appearing in the real fragments of Fig. 4(*c*). (There seem to be many ways of forming a trigonal prism!). These displacements are not the only ones taking place; at the same time, whole blocks must shear relative to each other to give the pattern shown in Fig. 4(*e*), which is a reconstruction of that of δ-Ni_2Si. This shearing also leads to the formation of other trigonal prisms between adjacent blocks through contacts which are marked with dotted lines in Fig. 4(*e*). Comparing again Figs. 4(*c*) and 4(*d*), one observes that these Ni—Ni distances are almost identical in both f.c.c. Ni and δ-Ni_2Si, and that these could serve as the hinges (dotted lines in Fig. 4*d*) around which the blocks have rotated to give the Ni_2Si structure. This rotation would occur at the same time that other bonds are broken or weakened and new ones are formed (those forming the trigonal prisms). It also seems that the formation of δ-Ni_2Si is a process in which only some of the original Ni—Ni bonds need to be broken in order to accommodate the Si atoms. The coordination number decreases from 12, in f.c.c. Ni, to 8 and 7 around Ni(1) and Ni(2), respectively, in the compound.

Concluding remarks

We have given four additional examples of compounds where fragments of the parent metal can easily be recognized. This leads us to substitute for the concept of clusters, that of a modified net of the parent metal, a concept which we believe has a more physical feel. In this context, the model of chemical twinning (Andersson & Hyde, 1974), used to describe some structures, is seen as just a structural feature derived from the modified parent metal and not as the intergrowth of two fragments related by a mirror plane. It should be added that the model of Andersson (1985) (see also Anderson & Hyde, 1989), describing complex structures as formed from fragments of other, less complicated, compounds, can be extended to simple structures. In the first stage, simple structures can be described as fragments of even simpler arrangements, *i.e.* those of the parent metals.

Another point of interest is that the structures just discussed, offer a new bridge between Solid State and Molecular Chemistry, in the sense that the distortions observed in the metal fragments do not seem to occur at random but obey correlations like those occurring in molecular compounds (Bürgi, 1975).

Finally, the ideas discussed here serve not only to describe structures in a simple way, but also to deduce plausible reaction mechanisms in the solid state as suggested by Andersson (1985) when describing complex structures. Deformation of metallic nets should obey the principle of least motion (Rice & Teller, 1938, 1939), as do reacting molecules, and a least-fragmentation principle could be considered as a new expression of the 'economy of nature'.

In memoriam of our colleague and friend Dr J. Lspez de Lerma. Work supported by CICYT, Spain, under project PB 90-0070.

References

ANDERSSON, S. (1985). *Structure and Bonding in Crystals*, edited by M. O'KEEFFE & A. NAVROTSKY, ch. 24. New York: Wiley.
ANDERSSON, S. & HYDE, B. G. (1974). *J. Solid State Chem.* **9**, 92–101.
ANDERSSON, S. & HYDE, B. G. (1989). *Inorganic Crystal Structures*. New York: Wiley.
ARONSSON, B. & RUNDQUIST, S. (1962). *Acta Cryst.* **15**, 878–887.
BÜRGI, H. B. (1975). *Angew. Chem. Int. Ed. Engl.* **14**, 460–473.
FRANZEN, H. F. (1978). *Prog. Solid State Chem.* **12**, 1–39.
HENDRICKS, S. B. & KOSTING, P. R. (1930). *Z. Kristallogr.* **74**, 511–533.
HUGHBANKS, T. (1989). *Prog. Solid State Chem.* **19**, 329–372.
JANSEN, M. (1987). *Angew. Chem. Int. Ed. Engl.* **26**, 1098–1110.
LANDOLT-BÖRNSTEIN (1971). *Structure Data of Elements and Intermetallic Phases*, New Series, Group III, Vol. 6, Part 5. Heidelberg: Springer-Verlag.
LIPSON, H. & PETCH, N. J. (1940). *J. Iron Steel Inst.* **142**, 95–106.
NAGAKI, D. A. & SIMON, A. (1990). *Acta Cryst.* C**46**, 1197–1199.
O'KEEFFE, M. & HYDE, B. G. (1981). *Structure and Bonding in Crystals*, edited by M. O'KEEFFE & A. NAVROTSKY, ch. 10. New York: Wiley.
O'KEEFFE, M. & HYDE, B. G. (1985). *Struct. Bonding (Berlin)*, **61**, 77–144.
PARTHÉ, E. (1981). *Structure and Bonding in Crystals*, edited by M. O'KEEFFE & A. NAVROTSKY, ch. 25. New York: Wiley.
RICE, F. O. & TELLER, E. (1938). *J. Chem. Phys.* **6**, 489–496.
RICE, F. O. & TELLER, E. (1939). *J. Chem. Phys.* **7**, 199.
SIMON, A. (1981). *Angew. Chem. Int. Ed. Engl.* **20**, 1–22.
SIMON, A. (1988). *Angew. Chem. Int. Ed. Engl.* **27**, 159–183.
TOMAN, K. (1952). *Acta Cryst.* **5**, 329–331.
VEGAS, A., ROMERO, A. & MARTÍNEZ-RIPOLL, M. (1990). *J. Solid State Chem.* **88**, 594–596.
VEGAS, A., ROMERO, A. & MARTÍNEZ-RIPOLL, M. (1991). *Acta Cryst.* B**47**, 17–23.
WELLS, A. F. (1975). *Structural Inorganic Chemistry*, 4th ed., ch. 29. Oxford: Clarendon Press.